Bone Reports 13 (2020) 100287

Contents lists available at ScienceDirect

Bone Reports

journal homepage: www.elsevier.com/locate/bonr

# The effect of age on the microarchitecture and profile of gene expression in femoral head and neck bone from patients with osteoarthritis

Dorit Naot[a,*], Maureen Watson[a], Ally J. Choi[a,1], David S. Musson[a], Karen E. Callon[a], Mark Zhu[a], Ryan Gao[a], William Caughey[b], Rocco P. Pitto[c], Jacob T. Munro[c], Anne Horne[a], Gregory D. Gamble[a], Nicola Dalbeth[a], Ian R. Reid[a], Jillian Cornish[a]

[a] Department of Medicine, University of Auckland, Private Bag 92019, Auckland 1142, New Zealand
[b] Middlemore Hospital, Counties Manukau District Health Board, Auckland 1062, New Zealand
[c] Department of Surgery, University of Auckland, Private Bag 92019, Auckland 1142, New Zealand

ARTICLE INFO

*Keywords:*
Bone microarchitecture
Ageing
Gene expression
Femur
Osteoarthritis

ABSTRACT

Ageing of the skeleton is characterised by decreased bone mineral density, reduced strength, and increased risk of fracture. Although it is known that these changes are determined by the activities of bone cells through the processes of bone modelling and remodelling, details of the molecular mechanisms that underlie age-related changes in bone are still missing. Here, we analysed age-related changes in bone microarchitecture along with global gene expression in samples obtained from patients with osteoarthritis (OA). We hypothesised that changes would be evident in both microarchitecture and gene expression and aimed to identify novel molecular mechanisms that underlie ageing processes in bone. Samples of femoral head and neck were obtained from patients undergoing hip arthroplasty for OA, who were either ≤60 years or ≥70 years of age. Bone microarchitecture was analysed in cores of trabecular bone from the femoral head (17 from the younger group and 18 from the older), and cortical bone from the femoral neck (25 younger/22 older), using a Skyscan 1172 microCT scanner (Bruker). Gene expression was compared between the two age groups in 20 trabecular samples from each group, and 10 cortical samples from each group, using Clariom S Human microarrays (ThermoFisher Scientific). We found no significant changes between the two age groups in indices of trabecular or cortical bone microarchitecture. Gene expression analysis identified seven genes that had higher expression in the older group, including the transcription factor *EGR1* and the glucose transporter *SLC2A3* (*GLUT3*), and 21 differentially expressed genes in cortical bone samples ($P < 0.05$, fold change > 2). However, none of the comparisons of gene expression had false discovery rate-adjusted $P < 0.1$. In contrast to our working hypothesis, we found only minor differences in gene expression and no differences in bone microarchitecture between the two age-groups. It is possible that pathological processes related to OA provide protection against age-related changes in bone. Our study suggests that in patients with OA, the bone properties measured here in femoral head and neck do not deteriorate significantly from the sixth to the eighth decade of life.

## 1. Introduction

Ageing is characterised by a progressive decline of physiological functions and increased susceptibility to chronic diseases. Based on experimental evidence, it is now widely accepted that physiological ageing results from non-adaptive processes and time-dependent accumulation of cellular damage (Farr and Almeida, 2018; Lopez-Otin et al., 2013). The number of research projects that focus on ageing processes has greatly increased in recent years, driven by the fact that elderly people represent the most rapidly growing segment of the population in most developed countries, and the experimental evidence suggesting that it might be possible to intervene medically to delay ageing.

Ageing processes in the skeleton lead to reduced bone mineral density (BMD) and decline in strength, and result in increased risk of

* Corresponding author.
*E-mail addresses:* d.naot@auckland.ac.nz (D. Naot), m.watson@auckland.ac.nz (M. Watson), jung.choi@uq.edu.au (A.J. Choi), d.musson@auckland.ac.nz (D.S. Musson), k.callon@auckland.ac.nz (K.E. Callon), mzhu031@aucklanduni.ac.nz (M. Zhu), r.pitto@auckland.ac.nz (R.P. Pitto), jacob.munro@auckland.ac.nz (J.T. Munro), a.horne@auckland.ac.nz (A. Horne), gd.gamble@auckland.ac.nz (G.D. Gamble), n.dalbeth@auckland.ac.nz (N. Dalbeth), i.reid@auckland.ac.nz (I.R. Reid), j.cronish@auckland.ac.nz (J. Cornish).
[1] Current address: Australian Institute for Bioengineering and Nanotechnology, The University of Queensland, Brisbane, Australia.

https://doi.org/10.1016/j.bonr.2020.100287
Received 18 March 2020; Received in revised form 26 May 2020; Accepted 2 June 2020
Available online 05 June 2020

fracture. The measurement of BMD is used to diagnose osteoporosis, a systemic skeletal condition associated with fragility fractures (Eastell et al., 2016; Liu et al., 2019). The most frequent sites of osteoporotic fractures are the hip, wrist, and spine; with hip fracture having the worst outcomes among osteoporotic fractures, causing morbidity and mortality in the elderly (Yang et al., 2009). Although BMD measurements are used to calculate fracture risk and inform decisions about preventative treatment, it is now well recognised that BMD is only one of many factors responsible for the increased risk of fracture in old age (Manolagas and Parfitt, 2010). In fact, most fragility fractures occur in individuals with BMD higher than the osteoporotic range (Pasco et al., 2006). Age itself has been identified as an independent risk factor, and it has been shown that at the same BMD, a 20-year increase in age increases the risk of fracture 4-fold (Hui et al., 1988). Additional factors that contribute to age-related increase in fracture risk can be broadly categorised as those that are extrinsic or intrinsic to bone. The main extrinsic factors are the drop in sex steroids, the decline in neuromuscular function, and the increased incidence of falls, with additional contribution of other age-related comorbidities (Marie, 2014). Intrinsic factors include changes in bone geometry, microarchitecture, and material properties that lead to reduced bone strength (Reeve and Loveridge, 2014; Zebaze et al., 2019). At a microstructural level, cortical bone has been shown to develop age-related increases in porosity, while in trabecular bone, reduced numbers and thinning of trabeculae have been demonstrated (Khosla, 2013).

Bone undergoes continuous remodelling through resorption of bone matrix by osteoclasts and formation of new matrix by osteoblasts. With age, the balance between the bone removed and new bone formed in the remodelling process becomes negative. Studies in mice and humans suggest that the age-related decline in bone quality results from attenuation of bone formation due to reduced differentiation of mesenchymal progenitor cells into osteoblasts and a decrease in osteoblast function (Marie, 2014). However, the molecular mechanisms, and in particular age-related changes in gene expression in bone cells that lead to these changes, are still largely unknown.

The current study aimed to identify local age-related changes in cortical and trabecular bone sampled from the proximal femur, a load-bearing site susceptible to fragility fractures. The samples were obtained from bone removed during hip replacement surgeries of patients with OA, who were either 60 years of age or younger, or 70 years of age or older. Bone microarchitecture and cortical bone tissue mineral density (TMD) were determined by microCT, and global analysis of gene expression was performed in order to identify potential underlying mechanisms that contribute to age-related changes in bone.

## 2. Materials and methods

### 2.1. Participants

This study was approved by the Northern X Regional Ethics Committee, and all participants provided written informed consent. Patients included in the study were undergoing total hip replacement surgeries for OA, and were aged either ≤60 years or ≥70 years. Exclusion criteria included the use of bone-active medications, metabolic bone disease, fracture of the hip to be replaced, renal impairment, untreated hypothyroidism or hyperthyroidism and malignancy within five years of enrolment.

### 2.2. Study design

Thirty participants were recruited from each age group. The two main end-points of the study were analysis of bone microarchitecture using microCT, and global analysis of gene expression using Clariom S Human microarrays (ThermoFisher Scientific). Trabecular and cortical bone sampled from the head and neck of femur, respectively, were used for microCT and gene expression analyses. In addition, BMD was measured by dual-energy X-ray absorptiometry (DXA) in a subgroup of participants. The number of participants and samples analysed by each method, and the overlap of these analyses are presented in Table 1 and Fig. 1.

**Table 1**
Number of participants or samples.

| | | ≤60 years | ≥70 years |
|---|---|---|---|
| Clinic visit (DXA) | | 10 | 12 |
| microCT | Trabecular bone | 17 | 18 |
| | Cortical bone | 25 | 22 |
| Gene expression | Trabecular bone | 20 | 20 |
| | Cortical bone | 10 | 10 |

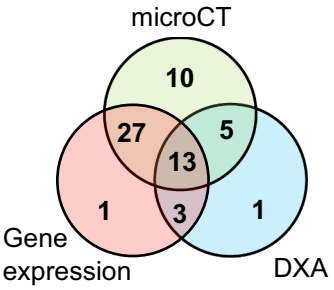


**Fig. 1.** Number of participants and samples analysed by the three methods The diagram presents the number of participants who had DXA scans, the number of samples analysed by microCT and gene expression microarrays, and the overlap among the three methods.

### 2.3. Bone mineral density

BMD of the lumbar spine (L1-L4), proximal femur, and total body was measured using a Lunar Prodigy dual-energy X-ray absorptiometer (GE Lunar, Madison, Wisconsin, USA).

### 2.4. Preparation of bone samples for microCT analysis and RNA extraction

Bone samples of head and neck of femur were collected and processed immediately following surgery. The samples from neck of femur, later used as a source of cortical bone, were taken before dislocation of the joint, in the anterior aspect of the junction between head and neck. Two cylinders of trabecular bone were extracted from the head of femur using a trephine. The trephine was positioned close to the femoral neck, to avoid sampling of subchondral bone. One trabecular sample was fixed in 70% ethanol at 4 °C, and later used for microCT analysis, and the second sample was processed for RNA extraction. In preparation for RNA extraction the thin cortex was removed, and trabecular bone was chopped to very small fragments using a scalpel, and washed several times in cold PBS, until it appeared free of blood and bone marrow contamination. The bone was processed in a Petri dish on top of a metal tray placed in ice, keeping the sample cold throughout the procedure, and then stored in liquid nitrogen. Cortical bone was obtained from the neck of femur. A ring of cortical bone was cut into sections, and trabecular bone removed using a bone Rongeur and a scalpel. Sections from the infero-posterior and infero-anterior regions of the cortical ring were fixed in 70% ethanol at 4 °C for microCT analysis, or snap frozen in liquid nitrogen for RNA extraction.

### 2.5. microCT analysis

Samples were rehydrated by soaking in PBS overnight, and scanned using a Skyscan 1172 microCT scanner (Bruker microCT, Aartselaar, Belgium), with X-ray voltage 80 kV and a 1 mm aluminium filter. After sample randomisation, scanning and analysis were performed in a

blinded fashion. The NRecon software was used for standardised reconstruction and the datasets were analysed using the CTAn software (Bruker microCT, Aartselaar, Belgium). Cores of trabecular bone were scanned with an isotrophic voxel size of 13 μm. Cylindrical volumes of interest of 6.40 mm diameter were created and analysed. The sections of cortical bone were cut, and uniform samples with cross-sections of 5 mm × 5 mm were scanned with an isotropic voxel size of 7 μm. For analysis, volumes of interest were created in regions with a clear cortical appearance, away from regions displaying trabecularisation. Tissue mineral density was calculated from measurements of X-ray attenuation of bone tissue, excluding the pores, and calibrated to hydroxyapatite standards.

### 2.6. RNA extraction

#### 2.6.1. Trabecular bone

Total RNA was extracted from approximately 100 mg of trabecular bone using the miRNeasy Mini Kit (Qiagen, Valencia, CA, USA). Frozen samples were ground to a powder using a mortar and pestle pre-cooled in liquid nitrogen, and the samples were immersed in liquid nitrogen throughout the grinding process. Bone powder was transferred to a tube with 4 mL QIAzol lysis reagent (Qiagen, Valencia, CA, USA), and homogenised using TissueRuptor® rotor-stator homogenizer (Qiagen, Hilden, Germany) with a disposable probe. For the next steps of RNA extraction we followed the miRNeasy Mini Kit protocol, including on-column DNaseI digestion, using a maximum of 50 mg starting bone material per column.

#### 2.6.2. Cortical bone

We tested a large number of RNA extraction methods, without success, before establishing the protocol below. Cortical bone fragments, stored in liquid nitrogen, were pulverised by cryogenic grinding in 6970 Freezer/Mill® (SPEX® SamplePrep, Metuchen, NJ). Approximately 100 mg of pulverised bone were mixed with 2.4 mL of TRI Reagent® (ZYMO Research Corp.) and placed on ice for 5 min. The suspension was passed 10 times through a 20-gauge needle attached to a sterile syringe, 0.48 mL of chloroform were added and mixed well, and tubes were incubated on ice for 5 min. After centrifugation at 12,000 rpm/4 °C/15 min, aqueous phase was transferred to a fresh tube, equal volume of TRI Reagent® added and mixed well, and tubes incubated on ice for 30 min. Equal volume of 100% ethanol was added to the samples, which were then loaded onto Zymo-Spin IICR columns (ZYMO Research Corp.) by repeated application of 700 μL of the mix. The Direct-zol™ RNA MiniPrep protocol was the followed, including on-column DNase I digestion.

RNA concentration and purity were determined using a NanoDrop 2000 spectrophotometer (ThermoFisher Scientific, Wilmington, DE, USA). RNA integrity was determined using the RNA ScreenTape Assay on TapeStation 4200 (Agilent Technologies, Santa Clara, CA, USA).

### 2.7. Gene expression analysis

RNA samples were used for global gene expression profiling on human Clariom™ S Assay microarrays (ThermoFisher Scientific, Wilmington, DE, USA). Gene expression was determined in 20 trabecular bone RNA samples from each age group. In the younger group, 10 samples were from females and 10 from males, and in the older group 12 samples were from females and 8 from males. Cortical gene expression was determined in 10 RNA samples (5 females and 5 males) from each age group. Sample preparation, microarray hybridisation, scanning and quality control were carried out at the Auckland Genomics Centre, Faculty of Sciences, University of Auckland.

#### 2.7.1. Contaminating cells of bone marrow origin in trabecular bone samples

In order to estimate bone marrow content in our trabecular bone samples, a list of 23 genes was constructed from the bone marrow transcriptome available on The Human Protein Atlas (Uhlen et al., 2015) (http://www.proteinatlas.org), and the geometric means were used to calculate a 'BM-content score' for each of the 40 samples. The samples were grouped into low-BM score, for samples with median score or below, and high-BM score for samples greater than the median score.

### 2.8. Statistical analysis

The statistical tests used are indicated in the figure legends. Transcriptome Analysis Console 4.0.2 (Affymetrix, Inc., Thermo Fisher Scientific) was used for quality control of the microarrays and statistical analysis of gene expression, including calculations of false discovery rate (FDR) and covariate analysis of BMI. The PANTHER classification system (Mi et al., 2019) was used for classification and enrichment analyses. GraphPad Prism 8.2.1 (GraphPad Software, La Jolla CA, USA), and SAS (v9.4, SAS Institute Inc., Cary, NC, USA) were used for all other statistical analyses. Tests were 2-tailed and a 5% significance level was maintained throughout the study.

## 3. Results

### 3.1. Characteristics of the study participants

The mean age, weight and BMI of the participants are presented in Table 2. Weight and BMI were significantly higher in the younger group. BMD was measured by DXA scans in a subgroup of 22 participants, 10 of whom were ≤60 years and 12 were ≥70 years of age. Thirteen participants (7 from the younger and 6 from the older age group) had their DXA scans prior to surgery, and nine (3 from the younger and 6 from the older age group) had the scans after they recovered from surgery. BMD values, T-scores, and *Z*-scores of the femoral neck, total hip, lumber vertebrae 1–4, and total body are presented in Fig. 2. Total body BMD and T-scores were significantly lower in the older age-group ($P = 0.040$ and $P = 0.043$, respectively), but after adjustment for BMI these differences did not remain significant ($P = 0.22$ for total body BMD and $P = 0.23$ for T-scores). One participant, a male from the younger age-group, had a lumbar spine T-score within the osteoporotic range, whereas the great majority of participants had BMD values within the normal range and T-score values above −1 in all four sites. The *Z*-scores were mostly above zero, and for all sites in the older group and total body in the younger group, the 95% CI did not include the value of Z-score = 0. In the lumber spine, the mean Z-score of the older group was higher than that of the younger group. It has been suggested that presence of osteophytes, mainly in the spine, can sometimes produce an artefact of increased BMD values.

### 3.2. Trabecular and cortical bone microarchitecture was similar in the two age-groups

Cylinders of trabecular bone were extracted from within the head of femur, away from the region of subchondral bone. Analysis of microCT scans of 17 samples obtained from the younger group and 18 samples

**Table 2**
Characteristics of the study participants.

| | ≤60 years[a] | ≥70 years[a] | Difference between means[b] |
|---|---|---|---|
| n (F/M) | 13/16 | 21/10 | – |
| Age (years) | 52.6 ± 6.5 | 77.3 ± 5.7 | 24.7 (21.5 to 27.8)* |
| Weight (kg) | 92.3 ± 20.7 | 71.3 ± 14.4 | 21.0 (11.8 to 30.2)* |
| BMI (kg/m$^2$) | 31.3 ± 6.7 | 26.3 ± 4.3 | 5.0 (2.1 to 8.0)* |

[a] Age, weight and BMI data are presented as mean ± SD.
[b] Presented as difference (95% CI).
* $P < 0.05$.

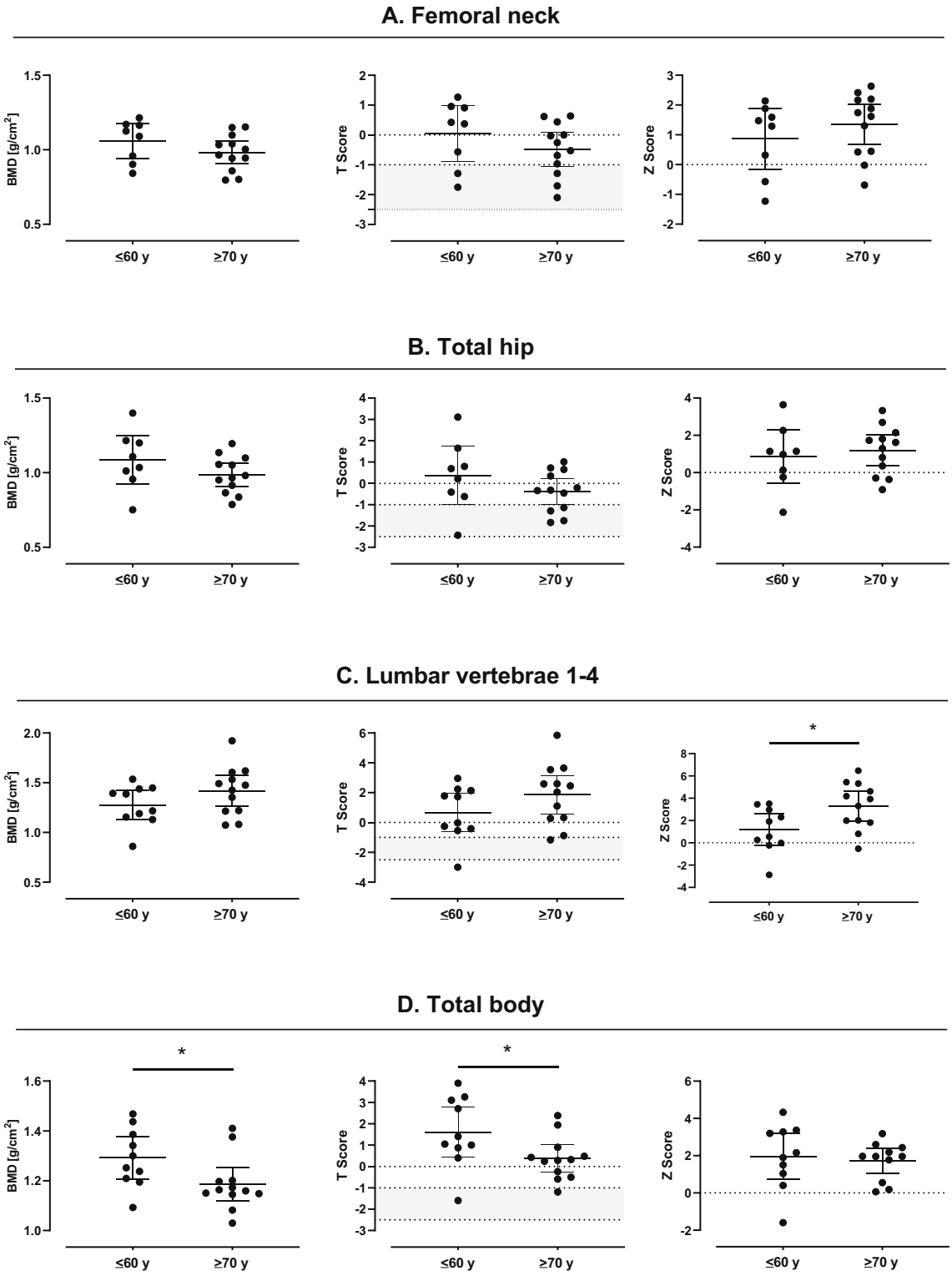


**Fig. 2.** BMD, T-scores, and Z-scores in the two age groups BMD values measured by DXA at four sites: femoral neck, total hip, L1–4 and total body, are presented on the left, the corresponding T-scores are in the middle, and Z-scores on the right. The graphs present individual values, group means, and 95% CI. The grey shaded area represents the osteopenic range. Samples were compared by *t*-test. *, $P < 0.05$, y: years.

from the older group found no significant differences between the group means in any of the four indices: bone volume (BV/TV), trabecular thickness, separation and number (Fig. 3). No significant differences between the age groups were found after adjustment for BMI.

Sections of cortical bone from the infero-anterior or infero-posterior regions of the femoral neck were analysed by microCT in 25 samples from the younger group and 22 samples from the older group. No significant differences between the group means were found in TMD and in three indices of cortical porosity: percentage volume of porosity, pore thickness, and pore connectivity density (Fig. 4). No significant differences between the age groups were found after adjustment for BMI.

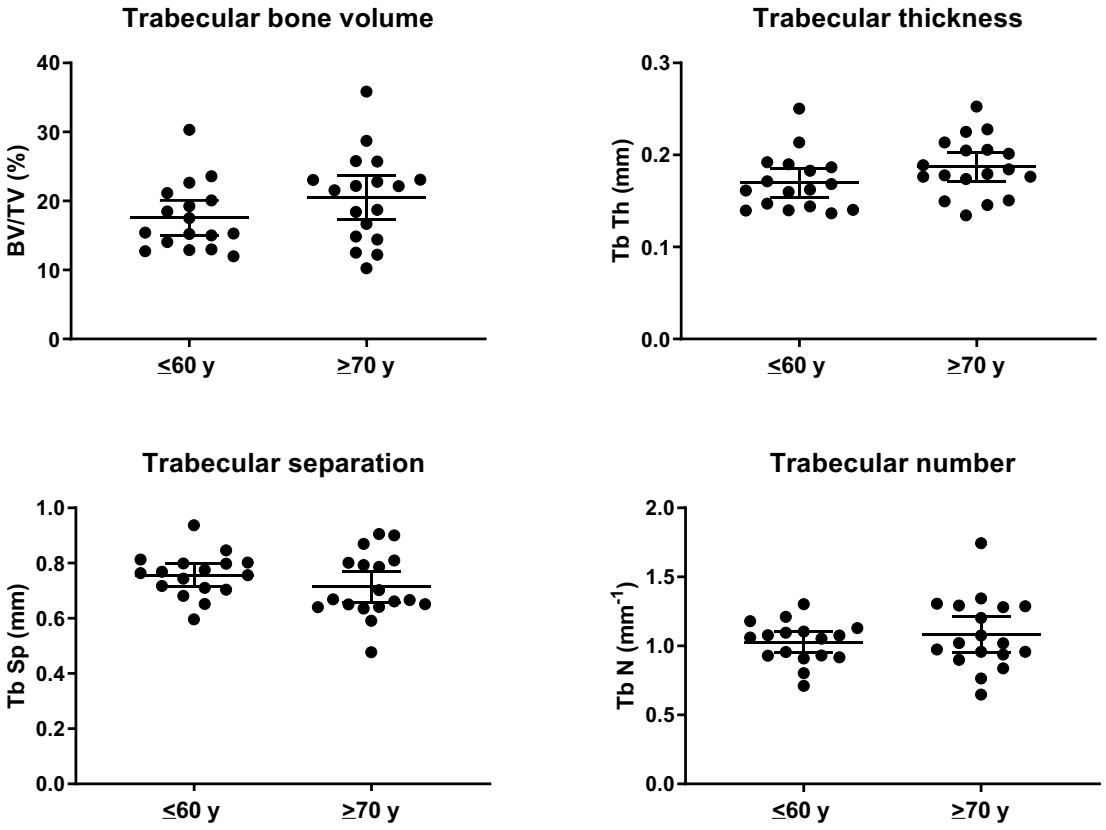


**Fig. 3.** MicroCT analysis of trabecular bone samples obtained from the femoral head The graphs present the value of each sample, the group means and 95% CI for the four trabecular bone indices indicated. No differences were found between the groups by Mann-Whitney test. y: years.

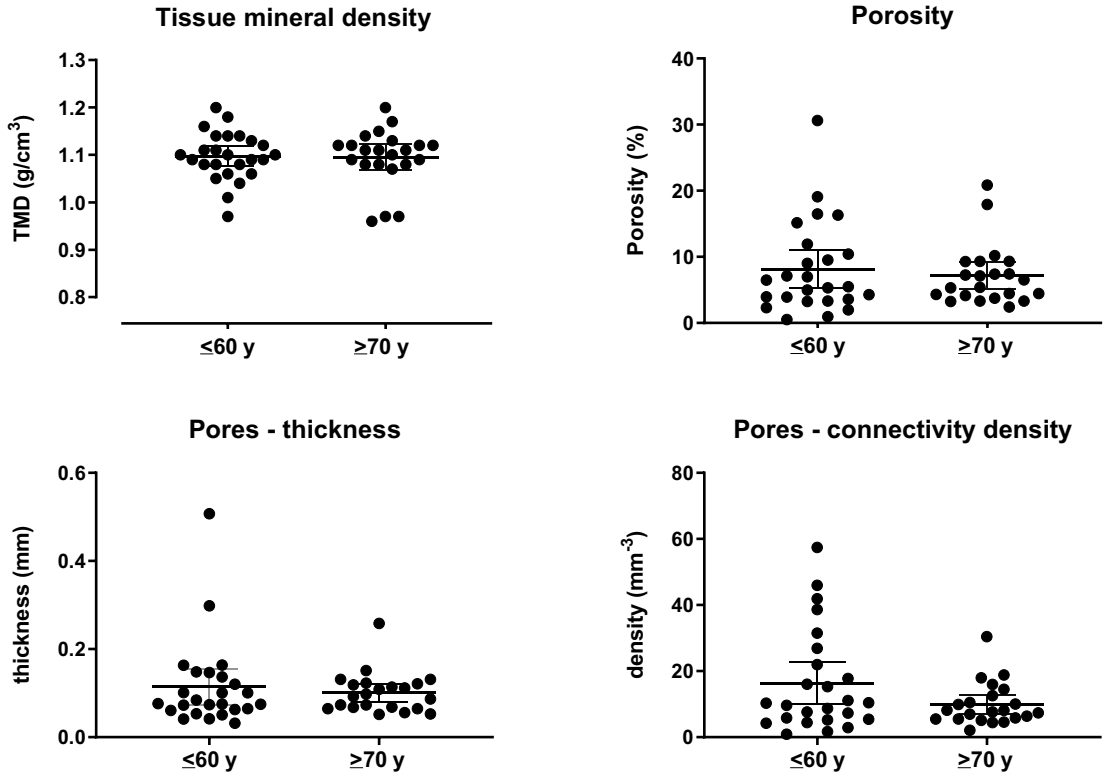


**Fig. 4.** MicroCT analysis of cortical bone samples obtained from the femoral neck Tissue mineral density and porosity were calculated from scans, porosity thickness and connectivity density were calculated from inverted microCT scans. The graphs present the value of each sample, the group means and 95% CI. No differences were found between the groups by Mann-Whitney test. y: years.

**Table 3**
Differentially expressed genes in trabecular bone samples (≥70 years vs. ≤60 years).

| | Gene symbol | Fold change | *P* value |
|---|---|---|---|
| 1 | *TIMD4* | 2.62 | 0.003 |
| 2 | *EGR1* | 2.60 | 0.027 |
| 3 | *SLC2A3* | 2.51 | 0.043 |
| 4 | *CCL18* | 2.39 | 0.042 |
| 5 | *MFAP5*[A] | 2.36 | 0.029 |
| 6 | *HLA-DQA1* | 2.10 | 0.019 |
| 7 | *FRZB*[A,B] | 2.09 | 0.029 |

[A] BMI-adjusted $P > 0.05$.
[B] BMI-adjusted fold-change < 2.

### 3.3. Gene expression analysis found only minor differences between the two age-groups

#### 3.3.1. Trabecular bone

Global gene expression was determined in 40 samples of RNA extracted from trabecular bone; 20 samples were from the younger group (10 females/10 males), and 20 from the older group (12 females/8 males). None of the comparisons had a FDR-adjusted $P < 0.1$. Only seven genes were differentially expressed above the threshold of fold change > 2 and unadjusted $P < 0.05$, all showing higher expression in the ≥70 years group (Table 3). When BMI was included as a covariate, only five of the genes remained significantly higher in the older group, with $P > 0.05$ for *FRZB* and *MFAP5*. Two genes of potential interest are *EGR1*, which encodes a transcription factor that plays a role in the regulation of cell proliferation and death (Thiel and Cibelli, 2002), and *SLC2A3* (*GLUT3*), one of the two principal transporters of glucose in osteoblasts (Lee et al., 2017).

The protocol for trabecular bone preparation included thorough rinsing with PBS until the samples appeared free of blood and bone marrow. However, residual contamination cannot be excluded, and presents a potential source of variability among RNA samples. Because this variability could mask true age-related differences in gene expression, we separated the samples into low- and high-BM content, as detailed in the Materials and Methods section, and compared between samples from participants ≥70 years and ≤60 years within each group. The low-BM content samples included 10 of the older and 12 of the younger group, and the high-BM content included 10 of the older and 8 of the younger group. None of the comparisons had an FDR-adjusted $P < 0.1$. Using the threshold of fold change > 2 and $P < 0.05$, 22 genes were differentially expressed in samples with low-BM score, and 38 genes in the high-BM score samples (Supplemental Tables S1A and S1B). Except for one gene (*F8*, coagulation factor VIII), there was no overlap between the gene lists. The low-BM score samples included two genes of interest: *ACP5* had lower level of expression in the older group and *IL6* had higher expression in the older group. *ACP5* encodes the osteoclast protein tartrate-resistant acid phosphatase, while the pro-inflammatory cytokine IL6 has well-established effects on bone metabolism (Sims, 2016) and has been implicated in ageing processes (Maggio et al., 2006). Differentially expressed genes in samples with high-BM score included *EGR1* and the Wnt pathway inhibitor, *FRZB*, with 7.0-fold and 5.1-fold higher expression in the older group, respectively. Several biological processes in the Gene Ontology database were overrepresented significantly (FDR $P < 0.05$) in the list of 38 genes from the high-BM score subset (Supplemental Table 2).

#### 3.3.2. Cortical bone

Global gene expression was analysed in 20 samples of RNA extracted from cortical bone; 10 samples were from the younger group and 10 from the older group, with five females and five males in each group. Similar to the trabecular bone gene expression analysis, none of the comparisons in cortical bone RNA had FDR-adjusted $P < 0.1$.

**Table 4**
Differentially expressed genes in cortical bone samples (≥70 years vs. ≤60 years).

| | Gene symbol | Fold change | P value |
|---|---|---|---|
| 1 | *LCA5L* | 2.14 | 0.0004 |
| 2 | *IL36G*[B] | 2.04 | 0.00006 |
| 3 | *LINC01587*[B] | 2.02 | 0.00005 |
| 4 | *EZR* | −2.01 | 0.024 |
| 5 | *NAIP*[A] | −2.01 | 0.039 |
| 6 | *ACTG1*[B] | −2.02 | 0.007 |
| 7 | *SCAP* | −2.03 | 0.00006 |
| 8 | *NUCB2*[B] | −2.08 | 0.002 |
| 9 | *CCL14* | −2.11 | 0.011 |
| 10 | *CYBRD1*[A,B] | −2.12 | 0.021 |
| 11 | *ARF4*[A,B] | −2.20 | 0.014 |
| 12 | *LINS1*[B] | −2.24 | 0.006 |
| 13 | *EPDR1*[A,B] | −2.26 | 0.021 |
| 14 | *GPX8*[A,B] | −2.28 | 0.003 |
| 15 | *SLC8A3* | −2.31 | 0.031 |
| 16 | *SERPINF1* | −2.37 | 0.010 |
| 17 | *APOD*[A] | −247 | 0.011 |
| 18 | *CD9*[A] | −2.54 | 0.014 |
| 19 | *COL24A1*[A] | −2.54 | 0.040 |
| 20 | *LOX* | −2.59 | 0.004 |
| 21 | *KDELR3* | −3.03 | 0.002 |

[A] BMI-adjusted P > 0.05.
[B] BMI-adjusted fold-change < 2 or > −2.

Twenty-one genes were differentially expressed (fold change > 2, P < 0.05), with four genes showing higher expression in the ≥70 years group (Table 4). When BMI was included as a covariate, only eight of the genes remained significantly different between the age-groups. One of these genes is *LOX*, which had 2.6-fold lower expression in the older group, and encodes the enzyme lysyl oxidase that catalyses the cross-linking of collagens and elastins and contributes to extracellular matrix stiffness (Vallet and Ricard-Blum, 2019). Statistical overrepresentation analysis did not identify any significant biological pathways in this list of genes.

### 3.4. Investigation of genes of interest

A list of 22 genes of interest was constructed, based on previous publications that found age-related changes in gene expression in bone. The list included specific osteoblast genes (*ALPL, BGLAP, COL1A1, COL1A2, IBSP, RUNX2* and *SP7*), osteocyte genes (*DMP1, FGF23, MEPE, PHEX* and *SOST*), the Wnt-signalling targets (*LEF1* and *TCF*), senescence markers (*FOXO3, RB1, SIRT1* and *TP53*) and genes of the Notch pathway (*HES1, HEY1, NOCTH1* and *NOTCH2*). The mean levels of expression of all 22 genes were similar between the two age groups (p > 0.05) in both trabecular and cortical bone.

In further testing of the 22 genes of interest, we extended our investigation beyond the question of age-related changes. Comparing the expression between trabecular and cortical bone, we found that in general, the pattern was similar – with high expression of *COL1A1*, *COL1A2*, *IBSP* and *RUNX2* (Fig. 5).

The relations between expression levels of the 22 genes and parameters of bone microarchitecture in individual participants were tested by Pearson correlation analysis. Correlations were tested between gene expression in trabecular samples and trabecular BV/TV, and between gene expression in cortical samples and values of cortical porosity, pore connectivity and TMD. Statistically significant correlations were found for five genes (Table 5). Expression of the senescence marker *TP53* was positively correlated with cortical porosity and connectivity. The Notch pathway gene *HEY1* was positively correlated with trabecular BV/TV, while *NOTCH2* expression was negatively correlated with cortical TMD. The osteocyte markers *DMP1* and *MEPE* showed negative correlation with cortical porosity, and *DMP1* was also negatively correlated with cortical connectivity. However, none of these correlations remained

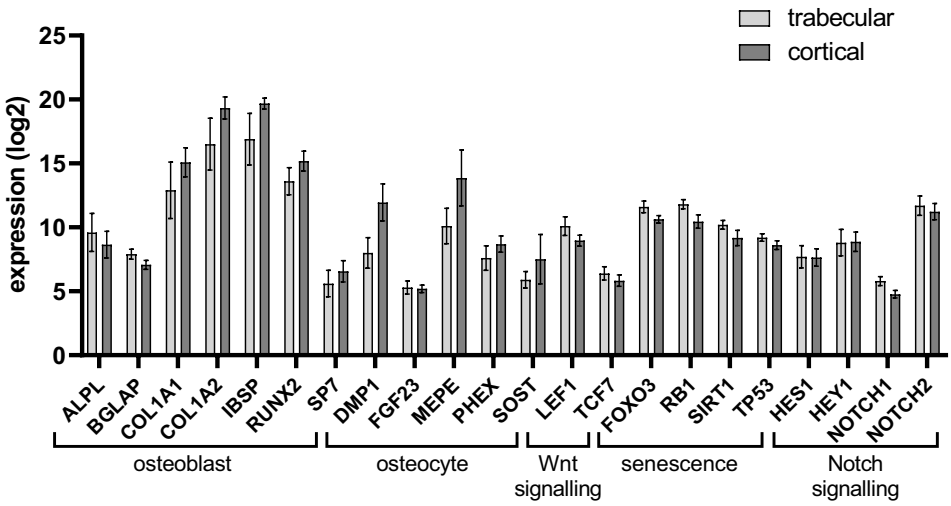


**Fig. 5.** Expression of candidate genes in RNA from trabecular and cortical bone samples The list of candidate genes was based on publications that found age-related changes in gene expression in bone. None of the genes was differentially expressed in the two age groups in our study, and therefore the two age groups for each type of bone were pooled. The bars represent the means ± SD of absolute expression values measured on the microarrays, $n = 40$ for trabecular bone, $n = 20$ for cortical bone.

**Table 5**
Correlation between expression of selected genes and microCT parameters[A].

| Gene[B] | | Trabecular | Cortical | | |
|---|---|---|---|---|---|
| | | BV/TV | Porosity | Connectivity | TMD |
| *TP53* | r | 0.20 | **0.53** | **0.60** | −0.33 |
| | P | 0.3 | **0.04** | **0.014** | 0.21 |
| *HEY1* | r | **0.45** | 0.046 | −0.16 | 0.29 |
| | P | **0.019** | 0.87 | 0.56 | 0.27 |
| *NOTCH2* | r | 0.13 | 0.09 | 0.02 | **−0.52** |
| | P | 0.53 | 0.73 | 0.94 | **0.04** |
| *MEPE* | r | 0.37 | **−0.50** | −0.47 | −0.19 |
| | P | 0.054 | **0.046** | 0.07 | 0.49 |
| *DMP1* | r | 0.33 | **−0.50** | **−0.57** | 0.12 |
| | P | 0.09 | **0.048** | **0.02** | 0.66 |

Statistically significant correlations appear in bold.

[A] Only samples analysed by both microCT and microarrays were included in the correlation analysis.

[B] No correlations were found for the following genes: *ALPL, BGLAP, COL1A1, COL1A2, IBSP, RUNX2, SP7, FGF23, PHEX, SOST, LEF1, TCF7, FOXO3, RB1, HES1, SIRT1, NOTCH2*.

significant after calculating FDR-adjusted *P* values to correct for multiple comparisons.

## 4. Discussion

Our study found only minor differences between bone samples from patients with OA who were aged 60 years or less and those who were aged over 70 years. MicroCT analysis of trabecular bone from the femoral head and cortical bone from the femoral neck found no age-dependent differences in either trabecular or cortical indices. All comparisons of gene expression between the two age-groups had FDR-adjusted $P > 0.1$. Further analysis, using a threshold of fold-change > 2 and unadjusted $P < 0.05$, identified seven genes that had higher expression in trabecular bone from the older group, and 21 genes that were differentially expressed in cortical bone. The results of the study were unexpected, as most previous studies found age-related deterioration of bone, and we anticipated that similar changes would be evident in our study group.

The current understanding of age-related microarchitectural deterioration of human bone is based on cross-sectional and longitudinal studies that used high-resolution peripheral quantitative computed tomography (HRpQCT), an imaging technique that allows in vivo non-invasive assessment of bone at peripheral skeletal sites, and on microCT analysis of bone samples ex-vivo. HRpQCT analysis of trabecular bone in the wrists of over 300 women between the ages of 20–90 years, found that trabecular number and BV/TV substantially decreased with age (Khosla et al., 2006). A later study focused on age-related changes in bone microarchitecture that were independent of BMD (Nicks et al., 2012). Participants under and over the age of 50 years were BMD-matched, and bone microstructure at the wrist was determined by HRpQCT. This study found increased cortical porosity, pore volume and pore diameter in the older group. Interestingly, in that study, age had no effect on trabecular bone microarchitecture. MicroCT analysis of trabecular bone samples from the femoral neck of patients between the ages of 60 and 90 years, found a decline of about 20% in BV/TV, with associated declines in trabecular number and thickness, and increase in separation (Chen et al., 2013; Chen et al., 2010). Linear, negative relation between trabecular BV/TV and age has also been demonstrated (Chen et al., 2013). In contrast, in a study that used a tissue sampling method similar to the one we used here, microCT analysis of trabecular bone in femoral heads from 37 participants aged 40–90 years found that the microarchitecture was unaffected by age (Perilli et al., 2007). The authors concluded that these findings are specific to patients with severe hip OA, and that OA pathology, directly or indirectly, protects against age-related deterioration of bone microarchitecture (Perilli et al., 2007).

Analysis of gene expression identified only minor differences between the age groups, and none of the comparisons had an FDR-adjusted $P < 0.1$, indicating that in this study group there were no strong candidates for age-related differentially expressed genes. The majority of prior studies of gene expression in human bone have used one of two sources: femoral head or neck from arthroplasties in patients with OA or following a fracture, or biopsies of the iliac crest taken from healthy donors (Farr et al., 2015; Reppe et al., 2017). The advantage of using iliac bone is that the donors are free of disease and can be recruited from a young adult age that is not represented in the OA group. However, obtaining the samples requires an invasive medical procedure in healthy volunteers, and because the iliac crest is not a load-bearing site it is less relevant than the femoral neck to studies of age-related changes that increase the risk of fracture. The main challenge in using femoral bone samples is that the group cannot be considered representative of the general population and conclusions are restricted to patients with OA or those who had a hip fracture. There is evidence to suggest that mechanisms that regulate bone turnover are altered in OA. A strong association between the ratio of RANKL/OPG mRNA and indices of bone turnover that was determined in trabecular bone samples from a control group, was not present in samples obtained from patients with OA (Fazzalari et al., 2001).

Most previous studies of gene expression in bone compared groups of patients with osteoporosis to patients with OA (Reppe et al., 2017).

The studies measured differential expression of mRNA or miRNA using quantitative RT-PCR, RT-PCR arrays, microarray or RNA sequencing. The number of participants varied from six to fifty in each group (Giner et al., 2013; Dragojevic et al., 2011). Two studies that focused on age-related changes in bone used iliac crest biopsies from healthy women (Farr et al., 2015; Roforth et al., 2014). The first study compared between 20 young (mean age, 30.0 years) and 20 older (mean age, 72.9 years) women, using a targeted-gene approach with quantitative RT-PCR. Of the 118 genes investigated, only one gene, the inhibitor of Wnt-signalling *SFRP1*, was found to be differentially expressed, with 1.6-fold increase in the older group (FDR $q < 0.05$) (Roforth et al., 2014). Interestingly, another member of the same group of Wnt pathway inhibitors, *FRZB* (alternative gene symbol *SFRP3*), was one of the seven genes that had higher expression in trabecular bone in the older group in our study (2.1-fold change, $P = 0.029$). However, *FRZB* expression was not significantly different between the groups after BMI-adjustment. A later study by the same group compared gene expression between 19 young women (mean age 30.3 years) and 19 older women (mean age 73.1 years), by RNA sequencing (Farr et al., 2015). Using a threshold of FDR $q < 0.05$, without restricting the comparison by fold-change, the study found 678 genes that were altered with age. Significant age-related alterations were identified in the Notch signalling pathway in both studies (Farr et al., 2015; Roforth et al., 2014). Age-related differences in genes of the Notch pathway were not found in our study, but interestingly, we found that the expression of the Notch pathway genes *HEY1* and *NOTCH2* were negatively correlated with trabecular BV/TV and cortical TMD, respectively.

A potential limitation of our study is that sample variability within each age-group contributed to the lack of separation between the two groups. The main sources of variability are the inclusion of females and males in the study and the consistency of the sampling sites. Although inclusion of females and males introduces heterogeneity within the groups, it provides a better representation of the population and accelerates the recruitment of participants for the study. Previous studies of microarchitecture and gene expression in human bone have used similar mixed groups (Perilli et al., 2007; Giner et al., 2013; Dragojevic et al., 2011; Hopwood et al., 2007). Reanalysing our microCT and trabecular gene expression results separately for males and females, did not identify significant differences between the age groups ($P > 0.05$ for microCT comparisons, and FDR-adjusted $P > 0.1$ for gene expression analysis, data not shown). The second potential source of variability is particularly important for the sampling of cortical bone, which is known to have marked regional heterogeneity in the femoral neck. Cortical bone in the superior region of the femoral neck is thinner than that in the inferior region, and in the elderly this regional variation is further accentuated with age-related thinning of the superior region and thickening of inferior cortices (Blain et al., 2008; Thomas et al., 2009). Although all the cortical samples that were analysed by microCT in our study were cut from the infero-anterior or infero-posterior regions of the femoral neck, we could not exclude slight variations in the sampling site, and therefore restricted our analyses to TMD and porosity, and did not include cortical thickness in this study. The difference in weight and BMI between the two groups is another potential limitation of our study. Although we used statistical tools to adjust for BMI, the possibility of a BMI-related metabolic variability between the groups cannot be excluded. However, this potential variability would have produced differences that are driven by metabolic state rather than age, and is less of a concern here as we found similar bone properties in the two groups. An additional limitation of our study is the fact that not all samples were analysed by all methods, potentially reducing the study power. Only 22 of the participants had a DXA scan, and a number of trabecular and cortical bone samples were structurally damaged and could not be used for microCT analysis. We also found that extracting good quality RNA from cortical bone was challenging and as a result the number of samples used in the microarray analysis was limited to 10 in each age group.

In summary, our study compared bone properties between two groups of patients with OA, a younger group of patients $\leq 60$ years and an older group of patients $\geq 70$ years of age, and found no differences between the group mean values of microarchitecture indices. Analysis of gene expression in bone cells found only minor differences between the groups. The findings were consistent in the different approaches we used to study bone properties and were similar for both trabecular and cortical bone, indicating that the two age-groups in our study were in fact similar to each other. We conclude that in people with OA, the bone properties determined here in the femoral head and neck do not deteriorate significantly from the sixth to the eighth decade of life. Alternative experimental strategies that can investigate bone properties in people who are free of joint disease might be better suited for the study of age-related deterioration of bone.

## Transparency document

The Transparency document associated with this article can be found, in online version.

## Conflicts of interest

None.

## CRediT authorship contribution statement

**Dorit Naot**:Conceptualization, Methodology, Formal analysis, Investigation, Data curation, Writing - original draft, Writing - review & editing, Supervision, Project administration, Funding acquisition.**Maureen Watson**:Methodology, Formal analysis, Investigation, Data curation.**Ally J. Choi**:Methodology, Investigation, Data curation.**David S. Musson**:Conceptualization, Investigation, Writing - review & editing.**Karen E. Callon**:Methodology, Investigation.**Mark Zhu**:Resources.**Ryan Gao**:Resources.**William Caughey**:Resources.**Rocco P. Pitto**:Conceptualization, Methodology, Resources.**Jacob T. Munro**:Conceptualization, Methodology, Resources.**Anne Horne**:Investigation, Resources, Data curation.**Gregory D. Gamble**:Methodology, Formal analysis, Writing - review & editing.**Nicola Dalbeth**:Resources, Writing - review & editing.**Ian R. Reid**:Conceptualization, Writing - review & editing, Funding acquisition.**Jillian Cornish**:Conceptualization, Writing - review & editing, Funding acquisition.

## Acknowledgements

This study was funded by the Health Research Council of New Zealand (Grant 15/576).

## Appendix A. Supplementary data

Supplementary data to this article can be found online at https://doi.org/10.1016/j.bonr.2020.100287.

## References

Blain, H., Chavassieux, P., Portero-Muzy, N., et al., 2008. Cortical and trabecular bone distribution in the femoral neck in osteoporosis and osteoarthritis. Bone 43, 862–868.
Chen, H., Zhou, X., Shoumura, S., Emura, S., Bunai, Y., 2010. Age- and gender-dependent changes in three-dimensional microstructure of cortical and trabecular bone at the human femoral neck. Osteoporos. Int. 21, 627–636.
Chen, H., Zhou, X., Fujita, H., Onozuka, M., Kubo, K.Y., 2013. Age-related changes in trabecular and cortical bone microstructure. Int. J. Endocrinol. 2013, 213234.
Dragojevic, J., Logar, D.B., Komadina, R., Marc, J., 2011. Osteoblastogenesis and adipogenesis are higher in osteoarthritic than in osteoporotic bone tissue. Arch. Med. Res. 42, 392–397.
Eastell, R., O'Neill, T.W., Hofbauer, L.C., et al., 2016. Postmenopausal osteoporosis. Nat Rev Dis Primers 2, 16069.

Farr, J.N., Almeida, M., 2018. The spectrum of fundamental basic science discoveries contributing to organismal aging. J. Bone Miner. Res. 33, 1568–1584.
Farr, J.N., Roforth, M.M., Fujita, K., et al., 2015. Effects of age and estrogen on skeletal gene expression in humans as assessed by RNA sequencing. PLoS One 10, e0138347.
Fazzalari, N.L., Kuliwaba, J.S., Atkins, G.J., Forwood, M.R., Findlay, D.M., 2001. The ratio of messenger RNA levels of receptor activator of nuclear factor kappaB ligand to osteoprotegerin correlates with bone remodeling indices in normal human cancellous bone but not in osteoarthritis. J. Bone Miner. Res. 16, 1015–1027.
Giner, M., Montoya, M.J., Vazquez, M.A., Miranda, C., Perez-Cano, R., 2013. Differences in osteogenic and apoptotic genes between osteoporotic and osteoarthritic patients. BMC Musculoskelet. Disord. 14, 41.
Hopwood, B., Tsykin, A., Findlay, D.M., Fazzalari, N.L., 2007. Microarray gene expression profiling of osteoarthritic bone suggests altered bone remodelling, WNT and transforming growth factor-beta/bone morphogenic protein signalling. Arthritis Res Ther 9, R100.
Hui, S.L., Slemenda, C.W., Johnston Jr., C.C., 1988. Age and bone mass as predictors of fracture in a prospective study. J. Clin. Invest. 81, 1804–1809.
Khosla, S., 2013. Pathogenesis of age-related bone loss in humans. J. Gerontol. A Biol. Sci. Med. Sci. 68, 1226–1235.
Khosla, S., Riggs, B.L., Atkinson, E.J., et al., 2006. Effects of sex and age on bone microstructure at the ultradistal radius: a population-based noninvasive in vivo assessment. J. Bone Miner. Res. 21, 124–131.
Lee, W.C., Guntur, A.R., Long, F., Rosen, C.J., 2017. Energy metabolism of the osteoblast: implications for osteoporosis. Endocr. Rev. 38, 255–266.
Liu, J., Curtis, E.M., Cooper, C., Harvey, N.C., 2019. State of the art in osteoporosis risk assessment and treatment. J. Endocrinol. Investig. 42, 1149–1164.
Lopez-Otin, C., Blasco, M.A., Partridge, L., Serrano, M., Kroemer, G., 2013. The hallmarks of aging. Cell 153, 1194–1217.
Maggio, M., Guralnik, J.M., Longo, D.L., Ferrucci, L., 2006. Interleukin-6 in aging and chronic disease: a magnificent pathway. J. Gerontol. A Biol. Sci. Med. Sci. 61, 575–584.
Manolagas, S.C., Parfitt, A.M., 2010. What old means to bone. Trends Endocrinol. Metab. 21, 369–374.
Marie, P.J., 2014. Bone cell senescence: mechanisms and perspectives. J. Bone Miner. Res. 29, 1311–1321.
Mi, H., Muruganujan, A., Huang, X., et al., 2019. Protocol update for large-scale genome and gene function analysis with the PANTHER classification system (v.14.0). Nat. Protoc. 14, 703–721.
Nicks, K.M., Amin, S., Atkinson, E.J., Riggs, B.L., Melton 3rd, L.J., Khosla, S., 2012. Relationship of age to bone microstructure independent of areal bone mineral density. J. Bone Miner. Res. 27, 637–644.
Pasco, J.A., Seeman, E., Henry, M.J., Merriman, E.N., Nicholson, G.C., Kotowicz, M.A., 2006. The population burden of fractures originates in women with osteopenia, not osteoporosis. Osteoporos. Int. 17, 1404–1409.
Perilli, E., Baleani, M., Ohman, C., Baruffaldi, F., Viceconti, M., 2007. Structural parameters and mechanical strength of cancellous bone in the femoral head in osteoarthritis do not depend on age. Bone 41, 760–768.
Reeve, J., Loveridge, N., 2014. The fragile elderly hip: mechanisms associated with age-related loss of strength and toughness. Bone 61, 138–148.
Reppe, S., Datta, H.K., Gautvik, K.M., 2017. Omics analysis of human bone to identify genes and molecular networks regulating skeletal remodeling in health and disease. Bone 101, 88–95.
Roforth, M.M., Fujita, K., McGregor, U.I., et al., 2014. Effects of age on bone mRNA levels of sclerostin and other genes relevant to bone metabolism in humans. Bone 59, 1–6.
Sims, N.A., 2016. Cell-specific paracrine actions of IL-6 family cytokines from bone, marrow and muscle that control bone formation and resorption. Int. J. Biochem. Cell Biol. 79, 14–23.
Thiel, G., Cibelli, G., 2002. Regulation of life and death by the zinc finger transcription factor Egr-1. J. Cell. Physiol. 193, 287–292.
Thomas, C.D., Mayhew, P.M., Power, J., et al., 2009. Femoral neck trabecular bone: loss with aging and role in preventing fracture. J. Bone Miner. Res. 24, 1808–1818.
Uhlen, M., Fagerberg, L., Hallstrom, B.M., et al., 2015. Proteomics. Tissue-based map of the human proteome. Science 347, 1260419.
Vallet, S.D., Ricard-Blum, S., 2019. Lysyl oxidases: from enzyme activity to extracellular matrix cross-links. Essays Biochem. 63, 349–364.
Yang, L., Peel, N., Clowes, J.A., McCloskey, E.V., Eastell, R., 2009. Use of DXA-based structural engineering models of the proximal femur to discriminate hip fracture. J. Bone Miner. Res. 24, 33–42.
Zebaze, R., Atkinson, E.J., Peng, Y., et al., 2019. Increased cortical porosity and reduced trabecular density are not necessarily synonymous with bone loss and microstructural deterioration. JBMR Plus 3, e10078.